

Hadronic Correlation Functions in the Interacting Instanton Liquid

T. Schäfer

*Institute for Nuclear Theory, Department of Physics, University of Washington,
Seattle, WA 98195, USA*

E.V. Shuryak

*Department of Physics, State University of New York at Stony Brook,
Stony Brook, NY 11794, USA*

Abstract

In this paper we study hadronic correlation functions in the interacting instanton liquid model, both at zero and nonzero temperature T . At zero T we investigate the dependence of the correlators on the instanton ensemble, in particular the effect of the fermionic determinant. We demonstrate that quark-induced correlations between instantons are important, especially in the repulsive η' and δ -meson channels. We also calculate a large number of mesonic and baryonic correlation functions as a function of temperature. We find three different types of behavior as $T \rightarrow T_c$. The vector channels ρ, a_1, Δ show a gradual melting of the resonance contribution and approach free quark behavior near the chiral phase transition. The light pseudoscalars and scalars π, σ , as well as the nucleon show stable resonance contributions, probably even surviving above T_c . Correlation functions in the heavy scalar channels η', δ are enhanced as $T \rightarrow T_c$.

11.30.Rd, 12.38.Lg, 12.38.Mh

Typeset using REVTeX

I. INTRODUCTION

Hadronic correlation functions provide a rich source of information about the spectrum of hadronic resonances and the interaction of quarks [1]. In this work we study the behavior of point-to-point QCD correlation functions $\Pi_h(x) = \langle j_h(x)j_h(0) \rangle$. Here, $j_h(x)$ is a current with the quantum numbers of some hadron h , and the averaging is performed over the QCD vacuum. For large euclidean separations $\tau = \sqrt{-x^2}$, the correlation function $\Pi_h(\tau)$ decays exponentially, the decay being controlled by the mass and the coupling constant of the lowest resonance in that channel. At small distances, asymptotic freedom implies that the correlator approaches free field behavior. The functional form at intermediate distances can be compared with the operator product expansion and reveals interesting information about the structure of the vacuum and the interactions between quarks.

In the present work we evaluate a large number of hadronic correlation functions, both at zero and non-zero temperature, in the interacting instanton liquid model (IILM) of the QCD vacuum. This study is a continuation of our earlier work on the instanton model [2–6], and we refer to these references, in particular [6], for a detailed description of the model, its underlying assumptions, and its theoretical and phenomenological foundations. The purpose of our study of hadronic correlation functions is twofold. First, we want to compare the correlation functions in the interacting ensemble with our results for the random one [4,5]. In the random model, the collective coordinates of the instantons are distributed randomly (except for their size, which is kept fixed), while in the interacting model, configurations are generated according to the correct measure, consisting of the bosonic contribution $\exp(-S)$ and, most important, the fermion determinant $\det(\hat{D} + m)$. This comparison is analogous to comparing “quenched” and “unquenched” lattice simulations (“quenching” means that the fermion determinant was neglected). The physical meaning of the quenched approximation and the role of quark induced correlations is an important problem [7,8]. We will argue that the fermion determinant indeed plays a very significant role, in particular in the pseudoscalar isosinglet (η' -meson) and scalar isovector (δ -meson) channels.

The second purpose of our work is to study the behavior of hadronic correlation functions at finite temperature. This study is clearly of great interest for the behavior of hadrons under extreme conditions, in particular near the chiral phase transition. In this regime there is little phenomenological information and lattice simulations have not yet progressed to the point that conclusive results can be obtained. It is therefore important to at least gain a qualitative understanding of the behavior of hadronic correlators near the phase transition. At finite temperature the role of the fermion determinant becomes even more significant. As discussed in [6], quark induced correlations drive the chiral phase transition in the instanton liquid. The mechanism for this transition is a rearrangement of the instanton liquid, going from a disordered instanton liquid to a phase of correlated instanton antiinstanton molecules.

Finally, we perform an exploratory study of correlators in QCD with many light flavors. QCD like theories with different matter content form a rich (and largely unexplored) field. In the instanton model, chiral symmetry is restored at large N_f . In order to improve our understanding of this unusual phase, we would like to study the hadronic spectrum in the large N_f instanton liquid.

The paper is organized as follows. In section 2 we calculate the hadronic correlation functions at zero temperature, study the dependence on the instanton ensemble and compare with phenomenological and lattice information. In section 3 we extend our model to finite temperature, considering correlators in the imaginary time direction. In section 4 we evaluate correlation functions in the spatial direction, related to the spectrum of screening masses at finite temperature. In section 5 we do a similar study for QCD with many light quark flavors. Our conclusions are summarized in section 6.

II. CORRELATION FUNCTIONS AT ZERO TEMPERATURES

Before we proceed to the instanton model, let us mention other sources of information about the behavior of hadronic correlation functions at zero temperature. General results as well as the available phenomenological information is summarized in the review [1]. Let us

again emphasize that point-to-point correlation functions are directly related to the spectrum of physical excitations, and any model describing hadronic states and interquark interactions should be tested against these results. Lattice measurements of point-to-point correlation functions were reported in [9–12], while our previous results based on the random ensemble (RILM) can be found in [4,5]. An analytical approach to the random ensemble was pioneered by Diakonov and Petrov [13], and the corresponding coordinate space correlation functions were recently reported in [14].

Comparing these works one should keep in mind that both the lattice results and the random instanton model are “quenched” calculations: they ignore quark-induced effects in the ensemble. On the other hand, lattice measurements of course contain a number of effects not accounted for in the instanton model, in particular confinement forces and perturbative interactions between quarks. Using a method called “cooling” one can also eliminate these effects on the lattice, while preserving instanton contributions. The correlation functions in the cooled ensemble were studied in [15].

The correlation function are evaluated using the quark propagator in a given configuration. For an isovector meson current $j_\Gamma = \bar{u}\Gamma d$ with the quantum numbers of the Dirac matrix Γ , the correlator is given by

$$\Pi_\Gamma^{I=1}(\tau) = \langle \text{Tr}[\Gamma S(0, \tau)\Gamma S(\tau, 0)] \rangle . \quad (1)$$

For isoscalar currents $j_\Gamma = \frac{1}{\sqrt{2}}(\bar{u}\Gamma u + \bar{d}\Gamma d)$, there is an additional disconnected contribution

$$\Pi_\Gamma^{I=0}(\tau) = \langle \text{Tr}[\Gamma S(0, \tau)\Gamma S(\tau, 0)] \rangle - \langle \text{Tr}[S(0, 0)\Gamma]\text{Tr}[S(\tau, \tau)\Gamma] \rangle . \quad (2)$$

Baryonic correlators are calculated in an analogous way from traces involving three fermion propagators [5]. The calculation of the propagator in the multi-instanton background is described in detail in [16]. The most important point is that the zero mode part of the Dirac operator is inverted exactly, implying that the instanton induced (’t Hooft) interaction between quarks is included to all orders. The averaging is performed over all configurations in a given ensemble (random, quenched or unquenched). This implies that while correlators

in the quenched ensemble only include diagrams in which the valence quarks (the quarks created by the source) interact via the 't Hooft interaction, the unquenched correlation functions also include vacuum bubbles to all orders in the interaction. Although this will in general affect all correlation functions, it is of particular importance in channels like the η' or the σ , where quarks can annihilate into the vacuum.

In the following, we will always normalize correlation functions to the corresponding free correlator,

$$\Pi_{\Gamma}^0(\tau) = \text{Tr}[\Gamma S_0(\tau)\Gamma S_0(-\tau)] \quad S_0(\tau) = \frac{\gamma_4}{2\pi^2} \frac{1}{\tau^3}, \quad (3)$$

If the ratio $R = \Pi_{\Gamma}(\tau)/\Pi_{\Gamma}^0(\tau) > 1$, we will refer to the correlator as attractive, while $R < 1$ corresponds to repulsive interactions. The aim of this paper is not to make large scale numerical calculations of masses and coupling constants of hadrons, but rather to study the differences between the correlation functions in the various ensembles. Nevertheless, in order to make quantitative statements we need to determine these observables. In practice, this is done using a simple “zero width pole plus continuum” model for the spectral functions. For a scalar meson, this corresponds to the following parametrization of the coordinate space correlator

$$\Pi_{\Gamma}(\tau) = \lambda_{\Gamma}^2 D(m_{\Gamma}, \tau) + \int_{s_0}^{\infty} ds \rho_0(s) D(\sqrt{s}, \tau). \quad (4)$$

Here, $\rho_0(s)$ is the free spectral function corresponding to the perturbative quark-antiquark bubble in the correlation function. The resonance mass m_{Γ} , coupling constant λ_{Γ} and continuum threshold s_0 are then extracted by fitting the parametrization (4) to the measured correlation function. Similar parametrizations for other mesonic and baryonic correlation functions are given in [4,5], and a brief summary of our conventions for the various currents and coupling constants involved is given in table 2.

In our previous work on the statistical mechanics of the instanton liquid [6] we have studied a number of different instanton ensembles and the dependence of bulk parameters on the underlying instanton interaction. Some of these parameters are summarized in table

1. The first column shows the results obtained in fully interacting simulations using the so called streamline interaction (SLI). The second column shows our results using the same interaction in the quenched approximation (for $N_f = 0$). While the streamline interaction has certain attractive features, it is not easily generalized to finite temperature. For this reason we have also studied the instanton ensemble using the ratio ansatz interaction (RAI). The corresponding (unquenched) results are shown in the third column while the last column shows the parameters of the random ensemble for comparison. We should also emphasize that all of these ensembles, with the exception of the random one whose parameters were determined phenomenologically, satisfy a number of low energy theorems for the topological susceptibility and fluctuations of the instanton number, that follow from the renormalization properties of QCD [6].

All dimensionful quantities (again with the exception of the random ensemble) are given in units of the (Pauli-Villars) regulator Λ . The value of Λ has to be fixed from some physical observable or by using the measured value of $\Lambda_{\overline{MS}}$. Since we need a prescription to compare quenched and unquenched ensembles and since the experimental accuracy of $\Lambda_{\overline{MS}}$ remains poor, we have chosen to fix the physical instanton density at $n^{-1/4} = 1$ fm. The corresponding scale parameters for the different ensembles are listed in table 1. These values have been used to convert the measured condensates into physical units, and will be used in the following to provide the physical scale for the measured coordinate space correlation functions.

Before we come to a more detailed discussion of the correlation functions we would like to discuss what differences between the correlation functions in the different ensembles one would expect on the basis of the global parameters listed in table 1. The random ensemble, which is the simplest example of a quenched ensemble, depends on only two parameters, the instanton density n and the diluteness $n\bar{\rho}^4$. Using the mean field approximation [2,13], the dependence of the quark condensate, the pion decay constant and the pion mass on these parameters is given by

$$\begin{aligned}
\langle \bar{q}q \rangle &\sim \sqrt{\bar{n}/\bar{\rho}}, \\
f_\pi^2 &\sim n\bar{\rho}^2 (1 + O(\log(\sqrt{n}\bar{\rho}^2))), \\
m_\pi^2 &\sim 1/(\sqrt{n}\bar{\rho}^3) (1 + O(\log(\sqrt{n}\bar{\rho}^2))).
\end{aligned}
\tag{5}$$

If one uses the instanton density in order to fix the overall scale, then we expect the pion decay constant to grow with the average instanton size, while the quark condensate and the pion mass drop. The quark constituent mass grows with the average size as $M \sim \sqrt{n}\rho$. We have checked these predictions against numerical calculations in the random ensemble and they agree fairly well. These calculations also show that most hadronic masses, in particular the rho meson, the nucleon and the delta do not scale like the constituent mass but are essentially independent of $\bar{\rho}$. This provides further evidence in favor of the hypothesis that these states are really bound in the instanton model. An exception is the a_1 meson, whose mass scales roughly like the constituent mass, and which is presumably unbound in our model.

We have calculated a large number of $I = 1$ and $I = 0$ mesonic correlators, as well as those for nucleons and Δ baryons. Some of the results are shown in fig.1 and the corresponding resonance parameters are summarized in table 3. All of the correlators were obtained in a system of 128 instantons in a volume $(3.00)^3 \times 4.74 \text{ fm}^4$, with quark masses $m_u = 0.1\Lambda$ and $m_s = 0.7\Lambda$. In fig.1 the phenomenological curves from [1] are given by solid lines, and the results from the random ensemble by the open triangles connected by dashed lines¹. Our results for the two interacting ensembles are shown by the solid (SLI) and open (RAI) data points.

¹The results for the random ensemble differ slightly from the ones reported in [4,5], mainly because they were obtained at a somewhat larger quark mass in a smaller volume. The parameters used here were chosen in order to facilitate comparison with the unquenched ensembles. For unquenched calculations, the time and storage requirements for generating the configurations limit us to smaller physical volumes.

In fig.1a, we show the pion (pseudoscalar $I = 1$) channel. Although all ensembles show a qualitatively similar behaviour, the results in the interacting ensembles lie systematically below the phenomenological curve. There are two reasons for this deviation. The first one is just a technical point: the light quark current masses in our simulations are on the order of 20 MeV, still significantly heavier than the physical value $(m_u + m_d)/2 \simeq 6$ MeV. Using $m_\pi \sim \sqrt{m}$, as suggested by the Gell-Mann, Oakes, Renner relation, one can extrapolate the pion mass to the physical value of the quark masses. The results are also given in table 3. We observe that the pion mass is smaller in the interacting ensembles. The results are consistent with the experimental value in the streamline ensembles (both quenched and unquenched), but clearly too small in the ratio ansatz ensemble. This is in agreement with the mean field result (5), and a reflection of the fact that the ratio ansatz ensemble is too dense.

The other point is that the pion coupling to the pseudoscalar current, λ_π , is related to the quark condensate and the pion decay constant $\lambda_\pi = \langle \bar{q}q \rangle / f_\pi$. Since the quark condensate in the unquenched ensembles is smaller as compared to the random one, λ_π is also reduced. This is a consequence of correlations among instantons and not captured by the mean field approximation.

The pion decay constant f_π can be determined in a number of different ways, either from λ_π using the measured quark condensate and the PCAC relation quoted above, from the pion contribution to the axial vector correlator, or from the off-diagonal pseudoscalar axialvector correlator [4]. All of these methods yield consistent results and we simply quote an average in table 3. The pion decay constant in the unquenched streamline ensemble is somewhat too small, while in the ratio ansatz ensemble it is clearly too large. The latter fact is again consistent with the mean field estimate (5) and related to the fact that the RAI ensemble is not as dilute as phenomenology demands.

In fig.1c we present the results for the isovector-vector and axialvector (ρ and a_1 meson) channels. These two correlation functions are not affected by instantons to first order in the instanton density. In this case the various ensembles lead to results that are fairly similar to each other. The rho meson mass in the unquenched ensemble is lighter than in

the random ensemble and now very close to the experimental value $m_\rho = 770$ MeV. Since the mass is essentially independent of the diluteness of the ensemble, the difference must be due to correlations among the instantons. How correlated instanton-antiinstanton pairs may generate an attractive interaction in the vector channel was discussed in [17]. The a_1 mass in the interacting ensembles, in particular ratio ansatz one, is too large as compared to the experimental value. As mentioned above, the a_1 is probably unbound in the instanton model and the observed behavior is simply due to the constituent mass being larger if the ensemble is very dense.

The situation is drastically different for the two most repulsive channels, the η' meson (the $SU_f(3)$ singlet pseudoscalar) and its chiral partner, the $I = 1$ scalar which we will denote by δ . In Fig.1(b,d) we show the correlation functions for the non-strange η current $j_{\eta_{ns}} = \frac{1}{\sqrt{2}}(\bar{u}\gamma_5 u + \bar{d}\gamma_5 d)$ and the δ current $j_\delta = \bar{u}d$. For the delta, we do not have a phenomenological curve, but instead show the lattice result [10].

Out of about 40 correlation functions calculated in the RILM [4,5], only the η' and δ were completely unacceptable (the dashed lines): these two correlation functions drop very rapidly with distance, and become negative at $x \sim 0.4$ fm. This behaviour is clearly incompatible with a normal spectral representation of the correlators. The results in the unquenched ensembles (closed and open points) significantly improve the situation. The reason for this behavior is related to the formation of instanton-antiinstanton pairs in the unquenched ensembles (or, more generally, to the screening of the topological charge). For both the δ and the η' the single instanton contribution is repulsive, but the contribution from pairs is attractive [17]. Only if correlations among instantons and antiinstantons are sufficiently strong, the correlators are prevented from becoming negative. Quantitatively, the δ and η_{ns} masses in the streamline ensemble are still too heavy as compared to their experimental values. In the ratio ansatz, on the other hand, the correlation even show an enhancement at distances on the order of 1 fm, and the fitted masses are too light. This shows that these two channels are very sensitive to the strength of correlations among instantons.

In table 4 we summarize our results for baryons. The nucleon parameters are not strongly affected by the choice of instanton ensemble. The main difference is that the nucleon coupling constants are somewhat smaller in the unquenched ensembles, an effect that is similar to the reduction in λ_π observed above. The behavior of the Delta correlation functions is similar to the ρ meson, with the Delta mass being reduced in the unquenched ensembles. This brings the measured Delta-nucleon mass splitting, which is too large in the random ensemble, closer to its experimental value.

To summarize the dependence of hadronic correlation functions on the instanton ensemble, we find that pion properties are mostly sensitive to global properties of the instanton ensemble, in particular its diluteness. Good phenomenology demands $\bar{\rho}^4 n \simeq 0.03$, as originally suggested in [2]. The properties of vector mesons and the Δ are essentially independent of the diluteness, but show some sensitivity to quark induced correlations. Correlations induced by the fermion determinant are extremely important in heavy scalar channels, like the η' and δ .

III. TEMPERATURE DEPENDENCE OF HADRONIC CORRELATION FUNCTIONS

In this section we would like to study the behavior of hadronic resonances as the temperature is raised and the system undergoes the chiral phase transition. The temperature dependence of mesonic susceptibilities, defined as integrated meson correlation functions, was already studied in [6]. The main conclusion in that work was that the transition is consistent with a nearby second order phase transition for $N_f = 2$. We could not conclusively settle the question of the fate of the $U(1)_A$ symmetry above the critical temperature of chiral symmetry restoration. Here, we want to study the nature of the transition in much more detail, by studying the behavior of hadronic correlation functions.

Clearly, the behavior of hadronic correlation functions is of great interest in connection with possible modifications of hadrons in hot and dense matter [18,19]. However, there

is very little phenomenological information about the behavior of hadronic correlators at nonzero temperature. One source of information is the Operator Product Expansion (OPE), but at $T \neq 0$ additional assumptions about the temperature dependence of the condensates are needed. Some consensus has emerged from the work on sum rules based on the OPE (see, for example [20–22]). For most correlation functions, the dominant power corrections are determined by the quark condensate, and there is a tendency for resonance masses and continuum thresholds to drop as chiral symmetry is restored. Recently, the first results² from lattice measurements of point-to-point correlation functions at $T \neq 0$ were published in [23].

At finite temperature, Lorentz invariance is broken, and the correlation functions in the spatial and temporal direction are independent. In addition to that, mesonic and baryonic correlation functions have to obey periodic or antiperiodic boundary conditions, respectively, in the temporal direction. In the case of spacelike correlators one can still go to large x and filter out the lowest exponents known as screening masses. While these states are of theoretical interest and have been studied in a number of lattice calculations, they do not correspond to poles of the spectral function in energy. In order to look for real bound states, one has to study temporal correlation functions. However, at finite temperature the periodic boundary conditions restrict the useful range of temporal correlators to the interval $\tau < 1/(2T)$ (about 0.6 fm at $T = T_c$), so that there is no direct procedure to extract information about the groundstate. The underlying physical reason is clear: at finite temperature excitations are always present. In the following we will study how much can be learned from temporal correlation functions in the interacting instanton liquid. In the next section we will also present the corresponding screening masses.

The calculation of the correlation functions at non-zero temperature is straightforward.

²There is a large amount of work on screening masses at finite T , which we will discuss in the next section.

As before, the correlators are determined from ensemble averages of various contractions of the quark propagator. The relevant instanton ensembles are the finite temperature ratio ansatz ensembles discussed in detail in [6]. The chiral phase transition in this ensemble occurs at $T \simeq 125$ MeV. The calculation of the quark propagator closely parallels the $T = 0$ case. The zero modes wave functions are substituted by their finite- T counterparts [24], and the non-zero mode part is summed over all fermionic Matsubara frequencies. As a result, the quark propagator obeys antisymmetric boundary conditions in the finite temperature box. Again, we normalize all correlation functions to the corresponding noninteracting correlators, calculated from the free propagator at finite temperature T

$$S_0(T, \tau) = \frac{\gamma_4}{2\pi^2} \sum_{n=-\infty}^{\infty} \frac{(-)^n}{(\tau + n/T)^3}. \quad (6)$$

Resonance parameters at finite temperature are extracted from a simple parametrization, analogous to the parametrization (4) discussed above. In the case of a scalar meson, it reads

$$\Pi_\Gamma(\tau) = \lambda_\Gamma^2 D(T, m_\Gamma, \tau) + \text{Tr}[\Gamma S^V(T, m, \tau) \Gamma S^V(T, m, -\tau)], \quad (7)$$

where $D(T, m, \tau)$ is the finite temperature massive boson propagator and $S^V(T, m, \tau)$ is the Dirac vector part of the finite T massive fermion propagator. The second term corresponds to the contribution of massive constituent quarks at finite temperature. As $m \rightarrow 0$, the continuum threshold moves down to zero energy.

The finite temperature temporal correlation functions in the interacting instanton liquid are presented in figs.2-5. In fig.2a,b we show the pion and sigma correlators for various temperatures. Here and in the following figures, open points correspond to temperatures below T_c , while the solid points show results near and above T_c . The π and σ correlators are larger than the perturbative one at all temperatures, implying that the interaction is attractive even above T_c . The peak height decreases strongly with T , but too a large part this is a simple consequence of the fact that the length of the temporal direction shrinks. Below T_c , the disconnected part of the sigma correlation functions tends to the square of the quark condensate at large distance. Above T_c , chiral symmetry is restored and the σ and π correlation functions become equal.

The vector and axial vector correlation functions are shown in fig.2(c,d). At low T the two are very different while above T_c they become indistinguishable, again in accordance with chiral symmetry restoration. In the vector channel, the changes in the correlation function indicate the “melting” of the resonance contribution. At low T (e.g. $T = 0.43T_c$, shown by the open triangles) one can see a peak in the correlation function at $x \simeq 1$ fm, indicating the presence of a bound state well separated from the two quark (or, more realistically, two pion continuum) continuum. However, this signal disappears at $T \sim 100\text{MeV}$, implying that the ρ meson coupling to local current becomes small. This is consistent with the idea that the resonance “swells” (or completely dissolves) in hot and dense matter. A similar phenomenon is also observed in the Delta baryon channel, see fig.3d. At $T = 0.43T_c$, there is a shoulder in the chiral even Delta correlation function Π_2^Δ , consistent with the presence of a bound state, but the signal completely disappears at $T = 0.86T_c$. Note however that in the instanton model, there is no confinement and the amount of binding in the ρ and Δ channel is presumably small. In full QCD, these two resonance might therefore be more stable as the temperature increases³.

The dominant effect at small temperature is mixing between the vector and axialvector channels [25]. This means, in particular, that there is a pion contribution to the vector correlator at finite T . This contribution is most easily observed in the longitudinal vector channel $\Pi_{44}^V(\tau)$ (note that in fig.2 we show the trace $\Pi_{\mu\mu}^V(\tau)$ of the vector correlator). We find a sizeable enhancement in this channel at $T = 77$ MeV, but the effect disappears at larger temperatures $T > 110$ MeV.

For $T > 110$ MeV both the ρ and Δ correlation functions are well described by a continuum contribution only, modeled by the propagation of two or three massive quarks. The temperature dependence of the effective quark mass extracted from fits to the correlators

³On the other hand, in the real world both particles have a significant width, even at zero temperature. The question whether they survive as (complex) poles will therefore be difficult to answer.

is shown in fig.4. We observe that the values determined from the ρ meson and Δ baryon channels are in very good agreement. Note that the effective quark mass does not vanish at $T = T_c$. This behavior does not contradict chiral symmetry restoration. The effective mass consist of two parts, a scalar component which does violate chiral symmetry and indeed disappears at the critical point, and a vector component which is not constrained by the symmetry. The scalar part is mostly due to spontaneous symmetry breaking in the random instanton liquid, while the vector component also receives contributions from nonzero modes in the molecular vacuum.

At this point, let us compare our results to those obtained on the lattice. Point-to-point correlation functions at $T \neq 0$ in the temporal direction were calculated by Boyd et al. [23]. The lattice used in this work has $N_\tau = 8$ points in time direction (and $N_\sigma = 16$), so the information is clearly very limited. Still, one observes that the vector correlation function behaves perturbatively (as two independently propagating quarks) while the pion one does not, even above T_c . If we normalize the correlators so that $\Pi_\pi(\tau)/\Pi_\rho(\tau) = 1$ at $\tau = 0$, then we find that at $\tau = 0.5T^{-1}$ (where the effect is maximal) and $\beta = 5.3$ (corresponding to $T \simeq 1.2T_c$) this ratio is $\Pi_\pi(\tau)/\Pi_\rho(\tau) \simeq (2 - 4)$. This can be compared to our results shown in fig.2, where at $T = 1.13T_c$ this ratio is about 1.5. So, the agreement is quite fair, taking into account that the lattice data were obtained with only 8 points in the temporal direction⁴.

In figure 3, we show our results for some of the baryon correlation functions. As explained in detail in [4], and summarized briefly in table 5, there are 6 nucleon and 4 delta correlation functions that can be constructed out of the two Ioffe currents for the nucleon and the unique delta current. Half of these correlators, $\Pi_{1,3,5}^N$ and $\Pi_{1,3}^\Delta$ are chiral odd and have to vanish as chiral symmetry is restored. $\Pi_{2,4}^N$ as well as $\Pi_{2,4}^\Delta$ are chiral even and may show resonance

⁴ And these 8 points, according to our model, represent gauge field configurations corresponding to instanton-antiinstanton molecules polarized in the temporal direction!

signals even as chiral symmetry is restored. Π_6^N , the chiral even, off-diagonal correlator of the two Ioffe currents is special. Chiral symmetry does not require it to vanish, but since the two currents have different $U(1)_A$ transformation properties, it is sensitive to $U(1)_A$ symmetry breaking [26].

The chiral-odd correlator Π_1^N is shown in fig.3a. Since it does not receive a contribution from free quark propagation, the correlation function (in our normalization) starts at 0 at $\tau = 0$. At small temperature, there is a large signal which is dominated by the nucleon contribution even at fairly small distances $\tau \simeq 0.3$ fm. In accordance with chiral symmetry restoration, this signal disappears as $T \rightarrow T_c$. In terms of the nucleon spectrum, there are several possible explanations for this behavior. If one includes the lowest positive (N^+) and negative parity (N^-) resonances in the spectral function, we have

$$\Pi_1^N(\tau) = (\lambda_1^{N^+})^2 m_{N^+} D(m_{N^+}, \tau) - (\lambda_1^{N^-})^2 m_{N^-} D(m_{N^-}, \tau), \quad (8)$$

where $\lambda_1^{N^\pm}$ is the coupling of the first Ioffe current to the positive/negative parity nucleon. This implies that the correlator can vanish either because (i) the masses go to zero $m_{N^+} = m_{N^-} = \dots = 0$, or (ii) the resonances decouple $\lambda_1^{N^+} = \lambda_1^{N^-} = \dots = 0$, or (iii) the parity partners become degenerate $m_{N^+} = m_{N^-}$, $\lambda_1^{N^+} = \lambda_1^{N^-}$ and their contributions to the correlator cancel each other.

In order to distinguish between these possibilities let us consider the chiral-even nucleon correlator Π_2^N (see fig.4b). There is an enhancement in Π_2^N , which is fairly stable as a function of temperature. Since both parity states contribute with the same sign to Π_2^N (see the summary in table 5), the possibility (ii) mentioned above does not seem likely. The correlation function Π_6^N shown in fig.4(c) is very large at low temperature, but strongly suppressed near and above the chiral phase transition. Similar to other correlation functions sensitive to the fate of the $U(1)_A$ symmetry, which we will discuss below, this phenomenon depends strongly on the value of the current quark masses. In order for Π_6^N to vanish, the contribution from different resonances have to cancel each other, suggesting the existence of degenerate states with different parity.

Clearly, the numerical values of the nucleon mass and its coupling constant are very interesting. Unfortunately, our ignorance concerning the form of the spectrum and the limited information provided by the temporal correlation functions makes it very difficult to provide a definite result. The discussion above clearly suggests that we should at least include two (opposite parity) resonances in addition to the continuum contribution. Furthermore, the masses seen in the scalar and vector channel are independent of each other. As a result, there are too many parameters in order to sufficiently constrain any fit. The correlation functions in the chiral odd channels $\Pi_{1,3,5}^N$ can be described both in terms of a dropping scalar mass, or using two (almost) degenerate states with different parity. The chiral even correlators $\Pi_{2,4}^N$ are somewhat more restrictive. We find that the correlation functions require a nucleon mass (or vector self energy) and coupling that is almost independent of temperature while the continuum threshold drops.

Let us finally discuss the fate of the $U(1)_A$ symmetry from the correlation functions in the mesonic sector. Here we consider the δ and η_{ms} channels, the $U(1)_A$ partners of π and σ . The temperature dependence of these correlation functions is shown in fig.5 (a,b). We remind the reader that the amount of repulsion in the δ and η_{ms} was too strong in the random model (dashed lines), but the behavior is improved in the interacting model. In contrast to the cases considered above in which correlation functions at finite temperature were reduced in magnitude, now one observes the opposite trend. As the temperature increases, the amount of repulsion is clearly reduced. This effect is more pronounced in the δ than in the η_{ms} channel, partly because the $T = 0$ ensemble is overcorrelated and produces an η_{ms} mass that is already too light.

The question of $U(1)_A$ restoration at $T = T_c$ (or above) can be studied by comparing the η and δ correlators with their $U(1)_A$ partners, the π and σ (shown in fig.2). A serious complication for this comparison is the strong dependence of the η and δ correlators on the current quark mass. In fig.5 (d) we show the δ correlator at fixed temperature $T = 0.86T_c$

for a number of different current quark masses⁵ $m = 5.2, 8.6, 13, 26$ MeV. For a very small quark mass $m = 5.2$ MeV (open triangles), there is a significant enhancement in the δ channel, which is indeed equal to that in the pion channel. This would imply chiral and $U(1)_A$ restoration. However, this is not a physical result, but a finite size effect. If the quark masses in a system with finite volume become too small, chiral (and $U(1)_A$) symmetry breaking are lost.

In order to be more quantitative one would like to determine the precise masses and coupling constants of the η_{ms} and δ . Again, given the restricted information available and the uncertainty concerning the form of the spectrum, it is hard to obtain reliable results for these parameters. In practice, we need to make some assumptions. Here, we first fix the non-resonant continuum, assuming it to be given by free propagation of quarks with the effective masses determined above. In the temperature region of interest, $T \geq 100$ MeV, the pion and delta masses are roughly consistent with zero $m_\pi \simeq m_\delta \simeq 0 \pm 200$ MeV. In the following we therefore fix the masses to be zero and study the temperature dependence of the coupling constants $\lambda_{\pi,\delta}$. In fig.5(c) we compare the coupling constants for the pion (stars) and delta. At $T = 130$ MeV we show the value of λ_δ for the different quark masses discussed above. For the lowest mass $m = 5.2$ MeV, the $U(1)_A$ symmetry is restored even below T_c , but this is definitely a finite size effect. For a somewhat larger mass $m = 8.6$ MeV, $U(1)_A$ symmetry appears to be restored at or just above T_c . At even larger current quark masses, no evidence for $U(1)_A$ restoration is seen. To settle this important question will require significantly larger simulations.

Possible experimental signatures of (partial) $U(1)_A$ chiral symmetry restoration were discussed in [27] and, more recently, in [28,29]. Basically, the idea is that if the η_{ms} becomes degenerate with the π at $T \simeq T_c$, one would expect a significant (low p_T) enhancement of η

⁵These numbers refer to the valence quark mass, used in the calculation of the fermion propagator. The sea quark mass, used in generating the instanton ensemble, was fixed at 13 MeV.

and η' production in relativistic heavy ion collisions. The more recent papers have pointed out two important experimental hints. First, as discussed in [29], the WA80 collaboration at CERN found a (modest) enhancement of the η/π^0 ratio in central relative to peripheral (or pp) collisions [30]. Furthermore, the enhancement of the low-mass dilepton production observed by the CERES [31] and Helios [32] collaborations could be explained in terms of the Dalitz decays of (more abundant) η' mesons [28]. To study these suggestions more quantitatively would not only require a better determination of the η_{ns} mass, but also an understanding of $\eta - \eta'$ mixing and η' absorption as a function of temperature.

Summarizing this section we find that many correlation functions⁶ (in the restricted range in which they are accessible at finite temperature) are remarkably smooth as a function of temperature, despite the fact that the vacuum fields and the quark condensate change significantly. Phenomenologically this means that the melting of resonances is compensated by the continuum threshold moving down in energy. Roughly speaking, we find three different types of behavior in chiral even correlators. In “attractive” channels, like the π and σ meson or the nucleon, resonance contributions seem to survive the phase transition. In channels that do not have strong interactions at $T = 0$ (like the ρ meson and the Δ), the resonances disappear quickly, and the correlators can be described in terms of free quark propagation with a certain effective chiral mass. Finally, the most dramatic change is seen in “repulsive” channels δ, η' , where most of the repulsive interaction disappears near the chiral phase transition.

IV. SCREENING MASSES

Correlation functions in the spatial direction can be studied at arbitrarily large distance, even at finite temperature. This means that contrary to the temporal correlators, the

⁶At least those correlation functions, that are not required by chiral symmetry to vanish at the phase transition.

corresponding spectrum can be determined with good accuracy. Although this spectrum is not directly related to the spectrum of physical excitations, the structure of spacelike screening masses is still of theoretical interest and has been investigated in a number of lattice [33,34] and theoretical [35–38] works.

At finite temperature, antiperiodic boundary conditions in the temporal direction require the lowest Matsubara frequency for fermions to be πT . This energy acts like a mass term for propagation in spatial direction, so quarks effectively become massive. At asymptotically large temperatures, quarks only propagate in the lowest Matsubara mode, and the theory undergoes dimensional reduction [39]. The spectrum of spacelike screening states is then determined by a 3-dimensional theory of quarks with chiral mass πT , interacting via the 3-dimensional Coulomb law and the nonvanishing spacelike string tension [40,41].

Dimensional reduction at large T predicts almost degenerate multiplets of mesons and baryons with screening masses close to $2\pi T$ and $3\pi T$. The splittings of mesons and baryons with different spin can be understood in terms of the nonrelativistically reduced spin-spin interaction. The resulting pattern of screening states is in qualitative agreement with lattice results even at moderate temperatures $T \simeq 1.5T_c$. The most notable exception is the pion, whose screening mass is significantly below $2\pi T$.

In this section we would like to study whether the spectrum of screening states can also be understood in the instanton liquid model. One should note that dimensional reduction does not naturally occur in the instanton model. Instantons have fermionic zero modes at arbitrarily large temperature, and the perturbative Coulomb and spin-spin interactions mentioned above are not included in our model.

The calculation of the spatial correlation functions is performed in the same way as described for the temporal correlators in the last section. Technically, there is no differences between the two cases, except that one has to make sure that there is no sensitivity to boundary effects in the spatial direction, while the boundary conditions in the temporal condition are of course essential.

We have not made an attempt to provide multi-parameter fits to the spatial correla-

tion functions. All we are interested in are the corresponding screening masses $\Pi(r) \xrightarrow{r \rightarrow \infty} \exp(-m_{scr}r)$. Our results are summarized in fig.6, where we have already normalized the data to the lowest fermionic Matsubara frequency πT . We find a picture that is qualitatively quite similar to our earlier work in the context of a schematic “cocktail” model (see fig. 11 of [17]), in which the instanton ensemble near T_c is described as a mixture of a random and a molecular instanton liquid.

First of all, the screening masses clearly show the restoration of chiral symmetry as $T \rightarrow T_c$: chiral partners like the π and σ or the ρ and a_1 become degenerate. Furthermore, the mesonic screening masses are close to $2\pi T$ above T_c , while the baryonic ones are fairly close to $3\pi T$, as expected. Most of the screening masses are shifted slightly upwards as compared to the most naive prediction. Considering the vector channels ρ, a_1, Δ , this shift corresponds to a residual “chiral quark mass” on the order of 120-140 MeV.

The most striking observation is the strong deviation from this pattern seen in the scalar channels π and σ , with screening masses significantly below $2\pi T$ near the chiral phase transition. This effect persists to fairly large temperature. We also find that the nucleon-delta splitting does not disappear at the phase transition, but decreases smoothly. We have also studied different components of the vector correlator. The results shown by the full points in fig.6 have been extracted from the trace of the vector correlator, $\Pi_{\mu\mu} \sim \exp(-m_\rho r)$. Alternatively, one can study the longitudinal $\Pi_{44} \sim \exp(-m_{\rho_4} r)$ or transverse $\Pi_{ii} \sim \exp(-m_{\rho_i} r)$ components of the vector correlator. The results are also shown in fig.6. We find that the longitudinal screening mass near the chiral phase transition is smaller than the transverse one, $m_{\rho_i} - m_{\rho_4} \simeq 100$ MeV. This result is in qualitative agreement with the prediction from dimensional reduction [38], but disagrees with the lattice calculation [33]. Note that in the limit of a dilute system of fully polarized molecules, ρ_4 is expected to be degenerate with the pion [17]. The presence of unpaired instantons, interactions among the molecules and deviations from complete polarization cause the pion to be significantly lighter than the longitudinal rho.

V. THE CHIRALLY SYMMETRIC PHASE IN MULTI-FLAVOR QCD

QCD like theories with different matter content form a rich field and an interesting testing ground for our understanding of nonperturbative phenomena in QCD. Significant progress in this direction has recently been made in supersymmetric extensions of QCD [42], where it has been possible to determine the critical number of flavors, such that chiral symmetry is restored in the ground state for $N_f > N_f^{crit}$. Furthermore, many interesting phenomena, like exact nonabelian dualities occur in theories with specific flavor content. In our previous work [6] we have studied the phase diagram of QCD with many flavors (in the instanton model). We found that chiral symmetry is restored in the groundstate for more than four light quark flavors (in the case $N_c = 3$). In this section we would like to study the properties of this new phase in more detail, by considering hadronic correlation functions.

One more reason to look into spectrum of multi-flavor QCD with a chirally symmetric groundstate is the fact that it might provide some insight into the spectrum of QCD above the phase transition. In the instanton model, the mechanism for the large N_f transition is very similar to the one that causes the phase transition at finite temperature, the formation of correlated instanton-antiinstanton pairs⁷. Although correlation functions in the temporal direction at finite T shed some light on the nature of hadronic excitations at large temperature, it is hard to extract definite results. In the chirally symmetric phase for large N_f , on the other hand, one can study correlation functions at large distances and the determination of the spectrum is comparatively easy.

In [6] we found that the critical number of massless flavors in the instanton model is close to $N_f = 4$. Here we will consider the case $N_f = 5$, in order to be sure to be in the chirally restored phase. In this case the instanton density is $n = 0.0097\Lambda^4$, significantly smaller than the $N_f = 2$ case studied above: adding more light quarks reduces the tunneling probability.

⁷The main difference is that now we consider $T=0$ case, so Lorentz invariance is not broken and there is no preferred direction for the formation of molecules.

In the following, we will study correlation functions as a function of x in units⁸ of Λ^{-1} . Since n in units of Λ^4 is so much smaller than before, the typical distance will be rather large.

The correlation functions are calculated as described in section 2. Some of the results are shown in fig.6. Despite the fact that the distance x is unusually large, the deviation of the correlators from free propagation of massless quarks is only at the 10% level. The results for the vector and axial vector currents (which we label, as in QCD, by ρ and a_1) are quite typical for most correlators, including baryons. The correlators are suppressed with respect to free propagation, and their functional form can be explained simply in terms of a nonzero quark mass. Furthermore, this quark mass is consistent with the input quark mass, there is no dynamical mass generation. The splitting between the ρ and a_1 correlators is also consistent with the symmetry breaking caused by the nonzero current masses.

The only channels that display a non-trivial behavior are the scalar and pseudoscalar mesons. In fig.6 we show the π and δ correlation functions, both of which show an attractive interaction. If we interpret this enhancement as in eq. (7) in terms of a resonance superimposed on a two-quark continuum, we find

$$m_\pi = (1.4 \pm 0.38)\Lambda, \quad \lambda_\pi = (0.24 \pm 0.05)\Lambda^2, \quad m_q = (0.10 \pm 0.1)\Lambda \quad (9)$$

$$m_\delta = (1.4 \pm 0.42)\Lambda, \quad \lambda_\delta = (0.22 \pm 0.05)\Lambda^2, \quad m_q = (0.13 \pm 0.1)\Lambda. \quad (10)$$

Again, the quark masses are consistent with the input current masses. Furthermore, the π and δ mesons appear to be degenerate. This is not unexpected in the multi-flavor theory, since in the absence of chiral symmetry breaking the $2N_f$ -leg 't Hooft vertex cannot directly contribute to a mesonic two point function. Thus, we conclude that the spectrum in this phase consists of a multiplet of weakly bound scalar-pseudoscalar resonances coupled to (almost) massless quarks. These states are of course not Goldstone modes, but massive states, bound by the molecule induced interaction. They are also not stable particles, but

⁸In principle one could fix units as in section 2 above, but since $N_f = 5$ QCD is not a physical theory, this would not make much sense.

resonances that decay into quarks.

VI. CONCLUSIONS AND DISCUSSION

In summary, we have studied hadronic correlation functions in the interacting instanton liquid. At zero temperature, we have considered the behavior of hadronic correlators in different instanton ensembles, in particular the influence of quenching on the hadronic spectrum. While there are some subtle differences in the pion and rho meson parameters⁹, the main effect of the fermion determinant is seen in the η' and δ mesons channels. These are the only channels in which the random model fails completely.

Correlations between instantons induced by the fermionic determinant weaken the strong repulsion observed in the quenched (and random) ensembles and clearly improve the description of these two channels. However, a quantitative description of the η' and δ masses depends on details of the instanton interaction that are not well determined (and understood). Correlations between instantons are somewhat too weak (and the η' too heavy) in the streamline ensemble, stabilized by the phenomenological core determined in our previous work, while the correlations are too strong (and the η' is too light) in the ratio ansatz ensemble. An important global parameter of the instanton liquid is its diluteness. Good phenomenology, in particular in the pion channel, requires the instanton liquid to be rather dilute $\bar{\rho}^4 n \simeq 0.03$. The streamline ensembles, both quenched and unquenched, approximately satisfy this requirement, while the ratio ansatz leads to an ensemble which is too dense.

We have also studied temporal and spatial correlation functions in the instanton vacuum at finite temperature. Both types of correlators clearly show the restoration of chiral sym-

⁹We should note, however, that the scale parameters in the quenched and unquenched ensembles differ significantly. The more accurate statement is therefore that most correlation functions in the quenched and unquenched ensembles only differ by a common change of scale.

metry at $T \simeq 125$ MeV. In the instanton liquid model, the mechanism for this transition is the formation of instanton-antiinstanton molecules. This implies that even above the chiral phase transition there is a significant density of instantons, and we can expect nonperturbative contributions to the correlation functions. We indeed find such effects, most notably in the temporal correlation functions of light scalar mesons. In channels like the π and σ we find stable resonance contributions that appear to survive the chiral phase transition. This result is in agreement with a recent lattice calculations of temporal correlators [23], where a similar enhancement in the scalar-pseudoscalar mesons channels in the chirally symmetric phase was observed.

Contrary to the light scalar mesons (and the nucleon channel), resonance contributions in the vector meson (and delta baryon) channels decrease very fast as the temperature increases. Above $T \simeq 100$ MeV, the correlation functions are consistent with free propagation of quarks with a nonvanishing chiral mass. This mass varies smoothly through the phase transition, and only disappears at significantly larger temperatures. Finally, in the heavy scalar meson channels, in particular the η' and δ , the strong repulsion seen at $T = 0$ disappears. Near the chiral phase transition, we observe some tendency toward $U(1)_A$ symmetry restoration. This result, however, depends very sensitively on the value of the current quark mass. A final verdict on the fate of $U(1)_A$ symmetry will therefore require detailed simulations in much larger volumes.

As already emphasized in the introduction, our study of correlation functions at finite temperature is qualitative in nature. We have been unable to give detailed numerical predictions of the temperature dependence of hadronic masses and coupling constants. This problem is related to the limited range covered by temporal correlation functions, our ignorance concerning the form of the spectral density, and the fact that more resonances need to be included at $T \neq 0$. It is a difficulty that our approach shares with other attempts, like QCD sum rules or the lattice, to determine the hadronic spectrum at finite temperature. Only more accurate results, the calculation of as many independent correlators as possible, and more theoretical work on possible modes of chiral restoration in the hadronic spectrum

will resolve this important question.

An example for the necessity to consider more than just one resonance is provided by the nucleon channel. We have considered six different nucleon correlation functions with different chiral symmetry properties. We conclude that, most likely, parity doubling plays a role in restoring the symmetry in the nucleon spectrum. The vector self energy stays roughly constant as a function of temperature, while it is difficult to observe a dropping scalar self energy.

In order to provide a more detailed comparison of our model with existing lattice calculations, we have also determined the spectrum of spacelike screening masses. The pattern of screening masses is much easier to determine than the spectral function in energy, and most mesonic and baryonic states at $T > T_c$ are close to simple multiples of the lowest Matsubara frequency πT . The most important exception are the light scalars π and σ , whose screening mass at T_c is only about half the naive value of $2\pi T$. We find a nonzero nucleon-delta splitting, as well as a splitting between the longitudinal and transverse components of the vector mesons. The latter appears to be reversed as compared to lattice simulations.

Finally, we have studied hadronic correlation function in QCD with many light flavors. This is a rich new field, that may provide many interesting lessons. Above a certain critical number of light flavors ($N_f^{crit} = 4$ in our case), chiral symmetry is restored even in the groundstate. In this case it is easier to determine the spectrum, since one can follow correlation functions to large distance. We find evidence of a (non Goldstone) “pion” resonance in multiflavor QCD, which is degenerate with the scalar sigma and delta mesons. Most likely, these mesons are organized in $U(N_f) \times U(N_f)$ multiplets. This strange world may offer some clues about the spectrum of ordinary QCD above the phase transition¹⁰.

¹⁰However, there are also important differences. For example, in multiflavor QCD the 't Hooft vertex has “too many legs”, so that it cannot contribute directly to meson correlation functions. We may therefore have a situation in which $U(1)_A$ symmetry is broken, but the η' is degenerate

VII. ACKNOWLEDGEMENTS

We would like to thank J. Verbaarschot for many useful discussions. This work was supported in part by US DOE grant DE-FG-88ER40388 and DE-FG06-90ER40561. Some of the numerical calculations were performed at NERSC, Lawrence Livermore Laboratory.

with the pion.

REFERENCES

- [1] E. V. Shuryak. *Rev. Mod. Phys.*, 65:1, 1993.
- [2] E. V. Shuryak. *Nucl. Phys.*, B203:93, 1982.
- [3] E. V. Shuryak. *Nucl. Phys.*, B302:559, 574, 599, 1988.
- [4] E. V. Shuryak and J. J. M. Verbaarschot. *Nucl. Phys.*, B410:55, 1993.
- [5] T. Schäfer, E. V. Shuryak, and J. J. M. Verbaarschot. *Nucl. Phys.*, B412:143, 1994.
- [6] T. Schäfer and E. V. Shuryak. *preprint, Stony Brook, SUNY-NTG-95-22*.
- [7] N. Dowrick and M. Teper. *Nucl. Phys. (Proc. Suppl.)*, B42:237, 1995.
- [8] P. Lacock and C. Michael. *Phys. Rev.*, D52:5213, 1995.
- [9] M. C. Chu, J. M. Grandy, S. Huang, and J. W. Negele. *Phys. Rev. Lett.*, 70:225, 1993.
- [10] M. C. Chu, J. M. Grandy, S. Huang, and J. W. Negele. *Phys. Rev.*, D 48:3340, 1993.
- [11] D. B. Leinweber. *Phys. Rev.*, D 51:6369, 1995.
- [12] D. B. Leinweber. *Phys. Rev.*, D 51:6383, 1995.
- [13] D. I. Diakonov and V. Yu. Petrov. *Nucl. Phys.*, B272:457, 1986.
- [14] M. Hutter. preprint, hep-ph/9501245.
- [15] M. C. Chu, J. M. Grandy, S. Huang, and J. W. Negele. *Phys. Rev.*, D49:6039, 1994.
- [16] E. V. Shuryak and J. J. M. Verbaarschot. *Nucl. Phys.*, B410:37, 1993.
- [17] T. Schäfer, E. V. Shuryak, and J. J. M. Verbaarschot. *Phys. Rev.*, D51:1267, 1995.
- [18] C. Adami and G. E. Brown. *Phys. Rep.*, 234:1, 1993.
- [19] G. E. Brown and M. Rho. *Phys. Rev. Lett.*, 66:2720, 1991.
- [20] A. I. Bochkarev and M. E. Shaposhnikov. *Nucl. Phys.*, B268:220, 1986.

- [21] V. L. Eletskii and B. L. Ioffe. *Phys. Rev.*, D51:2371, 1995.
- [22] T. Hatsuda, Y. Koike, and S. H. Lee. *Nucl. Phys.*, B394:221, 1993.
- [23] G. Boyd, S. Gupta, F. Karsch, and E. Laerman. *Z. Phys.*, C64:331, 1994.
- [24] B. Grossman. *Phys. Lett.*, A61:86, 1977.
- [25] M. Dey, V. L. Eletsky, and B. L. Ioffe. *Phys. Lett.*, B252:620, 1990.
- [26] T. Schäfer and E. V. Shuryak. *Phys. Lett.*, B356:147, 1995.
- [27] E. V. Shuryak. *Comm. Nucl. Part. Phys.*, 21:235, 1994.
- [28] J. Kapusta, D. Kharzeev, and L. McLerran. Preprint, to appear in *Phys. Rev. D*, 1995.
- [29] Z. Huang and X.-N. Wang. Preprint, to appear in *Phys. Rev. D*, 1995.
- [30] WA80 collaboration: A. Lebedev et al. *Nuc. Phys.*, A566:355c, 1994.
- [31] Ceres collaboration: G. Agakiechev et al. *Phys. Rev. Lett.*, 75:1272, 1995.
- [32] Helios collaboration: M. Masera. *Nuc. Phys.*, A590:93c, 1995.
- [33] C. De Tar and J. Kogut. *Phys. Rev.*, D36:2828, 1987.
- [34] A. Gocksch. *Phys. Rev. Lett.*, 67:1701, 1991.
- [35] V. L. Eletsky and B. L. Ioffe. *Sov. J. Nucl. Phys.*, 48:384, 1988.
- [36] T. H. Hansson and I. Zahed. *Nucl. Phys.*, B374:277, 1992.
- [37] V. Koch, E. V. Shuryak, G. E. Brown, and A. D. Jackson. *Phys. Rev.*, D46:3169, 1992.
- [38] T. H. Hansson, M. Sporre, and I. Zahed. *Nucl. Phys.*, B427:545, 1994.
- [39] T. Appelquist and R. D. Pisarski. *Phys. Rev.*, D23:2305, 1981.
- [40] C. Borgs. *Nucl. Phys.*, B261:455, 1985.
- [41] E. Manousakis and J. Polonyi. *Phys. Rev. Lett.*, 58:847, 1987.

[42] N. Seiberg. *Phys. Rev.*, D49:6857, 1994.

FIGURES

FIG. 1. Mesonic point-to-point correlation functions as a function of distance. All correlators are normalized to free quark propagation. Fig.1(a) shows the pseudoscalar (pion) correlator, (b) the isoscalar η_{ns} , (c) the vector and axialvector correlators (ρ, a_1) and (d) the isovector scalar (δ). The correlators are shown in different instanton ensembles, the unquenched streamline ensemble (solid points), the ratio ansatz ensemble (open points), and the random ensemble (dashed lines). The solid lines correspond to the phenomenological results, except for fig.1(d) which shows the result of a quenched lattice calculation.

FIG. 2. Temporal correlation functions at $T \neq 0$, normalized to free thermal correlators. Fig.2(a) shows the pseudoscalar (pion) correlator, (b) the isoscalar scalar σ , (c) the isovector axialvector (a_1) and (d) the isovector vector (ρ). Correlators in the chirally symmetric phase ($T \geq T_c$) are shown as solid points, below T_c as open points. The open triangles, squares and hexagons correspond to $T = 0.43, 0.60$ and $0.86 T_c$, while the closed triangles and squares show the data at $T = 1.00 T_c$ and $1.13 T_c$. For comparison we show the phenomenological $T = 0$ results from fig.1 (solid lines).

FIG. 3. Baryon temporal correlation functions at non-zero temperature. The curves are labeled as in Fig.2. Figures (a), (b) and (c) show the nucleon correlators Π_1^N, Π_2^N and Π_6^N . Figure (d) shows the chiral even Delta correlator Π_2^Δ .

FIG. 4. Temporal correlation functions at $T \neq 0$ for the nonstrange η (a) and the isovector scalar δ current (b). The curves are labeled as in fig.2,3. Figure (d) shows the scalar (δ) correlator at fixed temperature $T = 0.86 T_c$ for different quark masses, $m = 5.2, 8.6, 13, 26$ MeV, shown by open squares and triangles, closed squares and hexagons, respectively. In fig.(c) we show the value of the pseudoscalar and scalar coupling constants as a function of temperature. At $T = 0.86 T_c$ we show several values of $\lambda_\delta [\text{fm}^{-2}]$, corresponding to the different quark masses used in fig.(d).

FIG. 5. Effective ‘‘chiral’’ quark mass as a function of temperature T . The open (closed) points correspond to the values extracted from the Δ baryon and ρ meson correlators.

FIG. 6. Spectrum of spacelike screening masses as a function of temperature. The masses are given in units of the lowest fermionic Matsubara frequency πT .

FIG. 7. Correlation functions at zero temperature in $N_f = 5$ QCD. The correlators are normalized to free propagation and the distance is given in units of the scale parameter.

TABLES

	streamline	quenched	ratio ansatz	RILM
n	$0.174\Lambda^4$	$0.303\Lambda^4$	$0.659\Lambda^4$	1.0 fm^4
$\bar{\rho}$	$0.64\Lambda^{-1}$ (0.42 fm)	$0.58\Lambda^{-1}$ (0.43 fm)	$0.66\Lambda^{-1}$ (0.59 fm)	0.33 fm
$\bar{\rho}^4 n$	0.029	0.034	0.125	0.012
$\langle \bar{q}q \rangle$	$0.359\Lambda^3$ (219 MeV) ³	$0.825\Lambda^3$ (253 MeV) ³	$0.882\Lambda^3$ (213 MeV) ³	(264 MeV) ³
Λ	306 MeV	270 MeV	222 MeV	-

TABLE I. Bulk parameters of the different instanton ensembles.

channel	current	matrix element	experimental value
π	$j_\pi^a = \bar{q}\gamma_5\tau^a q$	$\langle 0 j_\pi^a \pi^b \rangle = \delta^{ab}\lambda_\pi$	$\lambda_\pi \simeq (480 \text{ MeV})^2$
	$j_{\mu 5}^a = \bar{q}\gamma_\mu\gamma_5\frac{\tau^a}{2}q$	$\langle 0 j_{\mu 5}^a \pi^b \rangle = \delta^{ab}q_\mu f_\pi$	$f_\pi = 93 \text{ MeV}$
δ	$j_\delta^a = \bar{q}\tau^a q$	$\langle 0 j_\delta^a \delta^b \rangle = \delta^{ab}\lambda_\delta$	
σ	$j_\sigma = \bar{q}q$	$\langle 0 j_\sigma \sigma \rangle = \lambda_\sigma$	
η_{ms}	$j_{\eta_{ms}} = \bar{q}\gamma_5 q$	$\langle 0 j_{\eta_{ms}} \eta_{ms} \rangle = \lambda_{\eta_{ms}}$	
ρ	$j_\mu^a = \bar{q}\gamma_\mu\frac{\tau^a}{2}q$	$\langle 0 j_\mu^a \rho^b \rangle = \delta^{ab}\epsilon_\mu\frac{m_\rho^2}{g_\rho}$	$g_\rho = 5.3$
a_1	$j_{\mu 5}^a = \bar{q}\gamma_\mu\gamma_5\frac{\tau^a}{2}q$	$\langle 0 j_{\mu 5}^a a_1^b \rangle = \delta^{ab}\epsilon_\mu\frac{m_{a_1}^2}{g_{a_1}}$	$g_{a_1} = 9.1$
N	$\eta_1 = \epsilon^{abc}(u^a C\gamma_\mu u^b)\gamma_5\gamma_\mu d^c$	$\langle 0 \eta_1 N(p, s) \rangle = \lambda_1^N u(p, s)$	
N	$\eta_2 = \epsilon^{abc}(u^a C\sigma_{\mu\nu}u^b)\gamma_5\sigma_{\mu\nu}d^c$	$\langle 0 \eta_2 N(p, s) \rangle = \lambda_2^N u(p, s)$	
Δ	$\eta_\mu = \epsilon^{abc}(u^a C\gamma_\mu u^b)u^c$	$\langle 0 \eta_\mu N(p, s) \rangle = \lambda^\Delta u_\mu(p, s)$	

TABLE II. Definition of various currents and matrix elements used in this work.

		streamline	quenched	ratio ansatz	RILM
m_π	[GeV]	0.265	0.268	0.128	0.284
m_π (extr.)	[GeV]	0.117	0.126	0.067	0.155
λ_π	[GeV ²]	0.214	0.268	0.156	0.369
f_π	[GeV]	0.071	0.091	0.183	0.091
m_ρ	[GeV]	0.795	0.951	0.654	1.000
g_ρ		6.491	6.006	5.827	6.130
m_{a_1}	[GeV]	1.265	1.479	1.624	1.353
g_{a_1}		7.582	6.908	6.668	7.816
m_σ	[GeV]	0.579	0.631	0.450	0.865
m_δ	[GeV]	2.049	3.353	1.110	4.032
$m_{\eta_{ms}}$	[GeV]	1.570	3.195	0.520	3.683

TABLE III. Meson parameters in the different instanton ensembles. All quantities are given in units of GeV. The current quark mass is $m_u = m_d = 0.1\Lambda$. Except for the pion mass, no attempt has been made to extrapolate the parameters to physical values of the quark mass.

		streamline	quenched	ratio ansatz	RILM
m_N	[GeV]	1.019	1.013	0.983	1.040
λ_N^1	[GeV ³]	0.026	0.029	0.021	0.037
λ_N^2	[GeV ³]	0.061	0.074	0.048	0.093
m_Δ	[GeV]	1.428	1.628	1.372	1.584
λ_Δ	[GeV ³]	0.027	0.040	0.026	0.036

TABLE IV. Baryon parameters in the different instanton ensembles. All quantities are given in units of GeV. The current quark mass is $m_u = m_d = 0.1\Lambda$.

correlator	definition	resonance contribution	$SU(2)_A$	$U(1)_A$
$\Pi_1^N(x)$	$\langle tr(\eta_1(x)\bar{\eta}_1(0)) \rangle$	$ \lambda_1^{N+} ^2 m_{N+} - \lambda_1^{N-} ^2 m_{N-}$	no	no
$\Pi_2^N(x)$	$\langle tr(\gamma \cdot \hat{x} \eta_1(x)\bar{\eta}_1(0)) \rangle$	$ \lambda_1^{N+} ^2 + \lambda_1^{N-} ^2$	yes	yes
$\Pi_3^N(x)$	$\langle tr(\eta_2(x)\bar{\eta}_2(0)) \rangle$	$ \lambda_2^{N+} ^2 m_{N+} - \lambda_2^{N-} ^2 m_{N-}$	no	no
$\Pi_4^N(x)$	$\langle tr(\gamma \cdot \hat{x} \eta_2(x)\bar{\eta}_2(0)) \rangle$	$ \lambda_2^{N+} ^2 + \lambda_2^{N-} ^2$	yes	yes
$\Pi_5^N(x)$	$\langle tr(\eta_1(x)\bar{\eta}_2(0)) \rangle$	$\lambda_1^{N+} (\lambda_2^{N+})^* m_{N+} - \lambda_1^{N-} (\lambda_2^{N-})^* m_{N-}$	no	no
$\Pi_6^N(x)$	$\langle tr(\gamma \cdot \hat{x} \eta_1(x)\bar{\eta}_2(0)) \rangle$	$\lambda_1^{N+} (\lambda_2^{N+})^* + \lambda_1^{N-} (\lambda_2^{N-})^*$	yes	no

TABLE V. Definition of various nucleon correlation functions. We also give the form of the resonance contribution (with the propagators suppressed) and the invariance properties under chiral $SU(2)_A$ and $U(1)_A$ transformations.

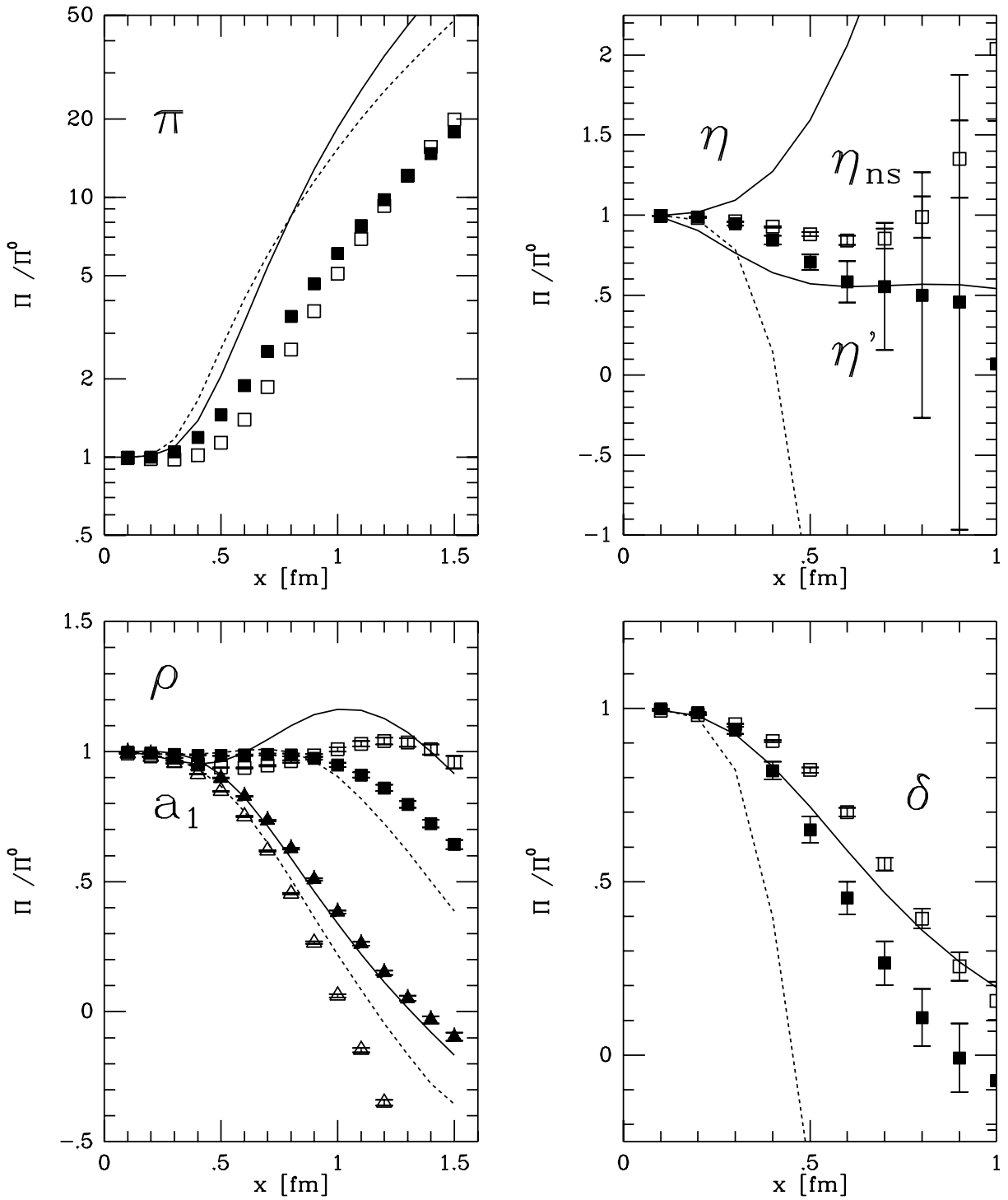


FIG. 1.

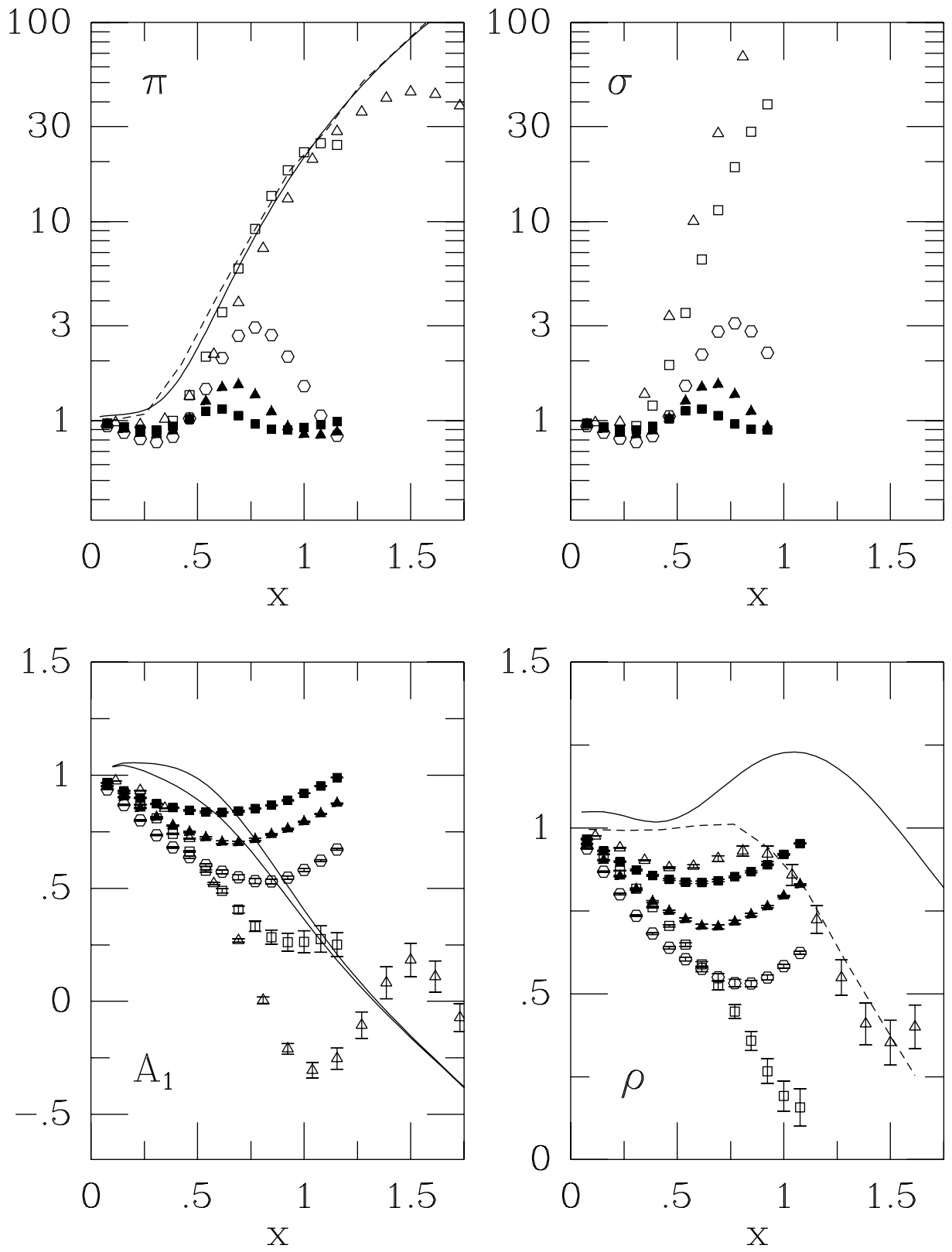


FIG. 2.

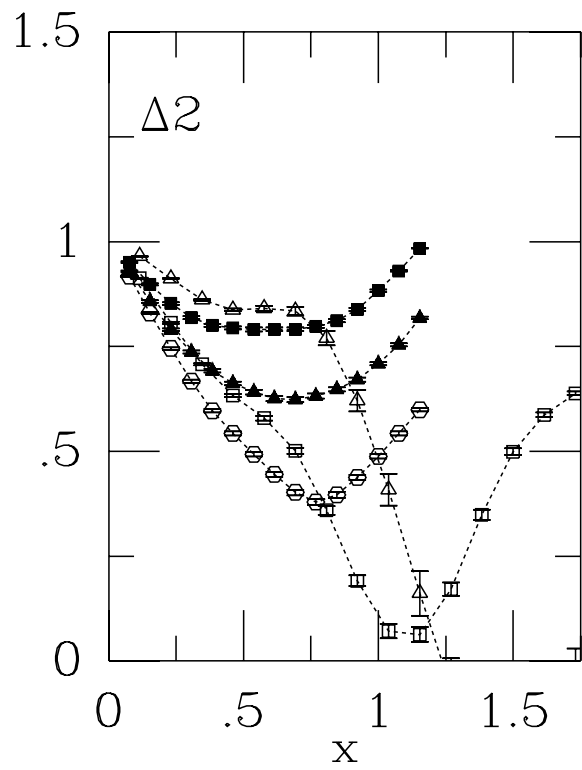
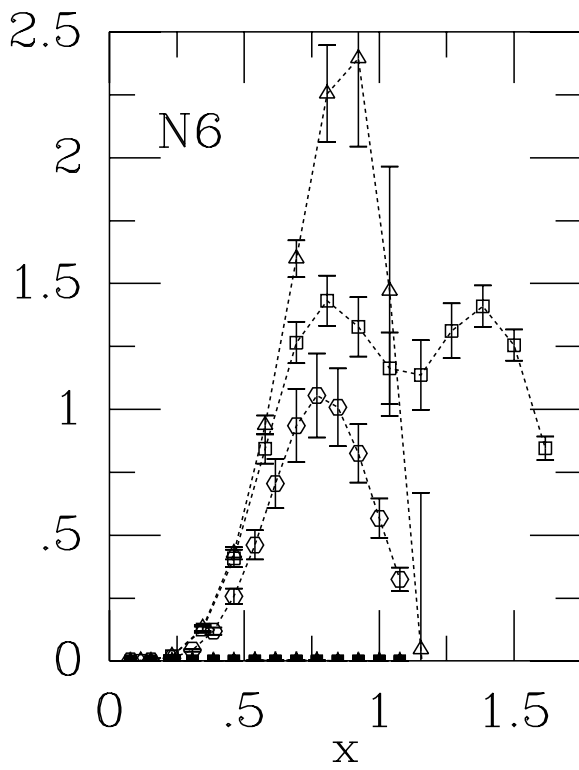
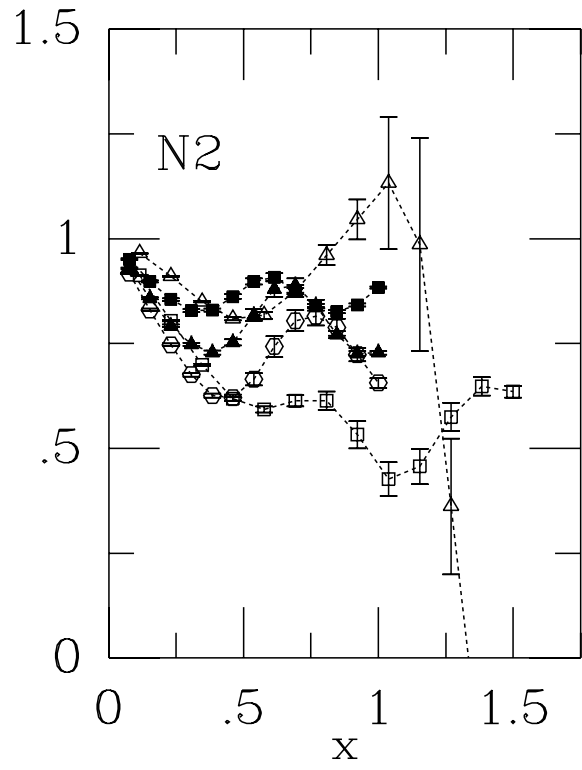
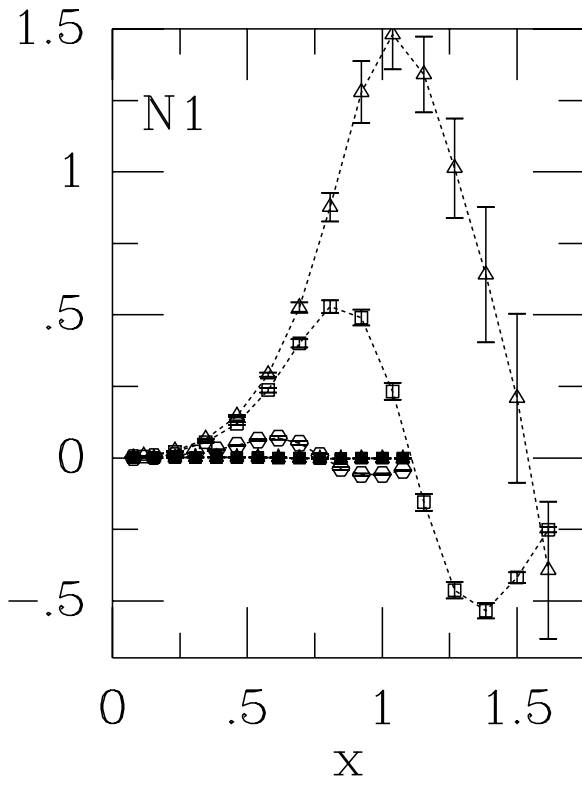


FIG. 3.

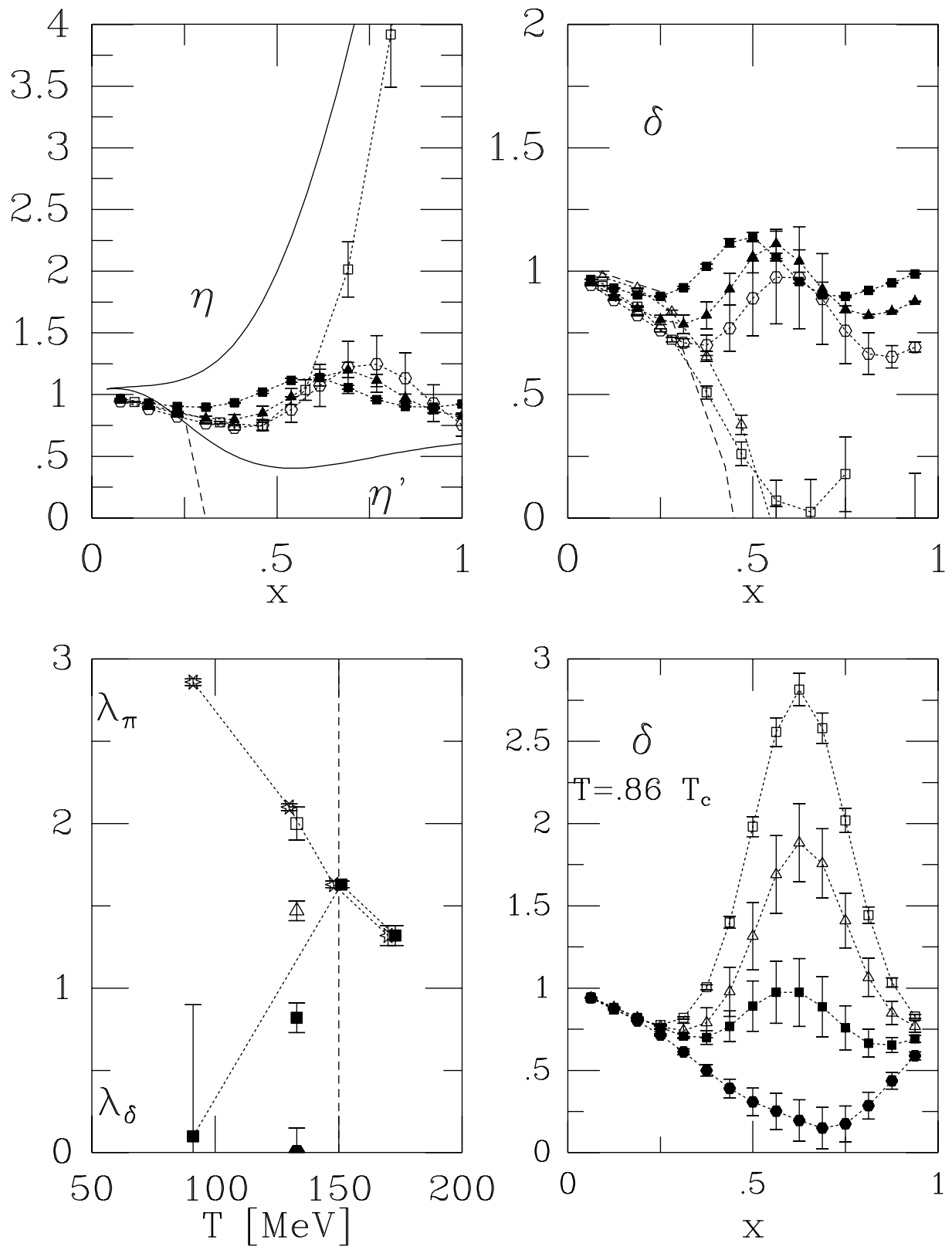


FIG. 4.

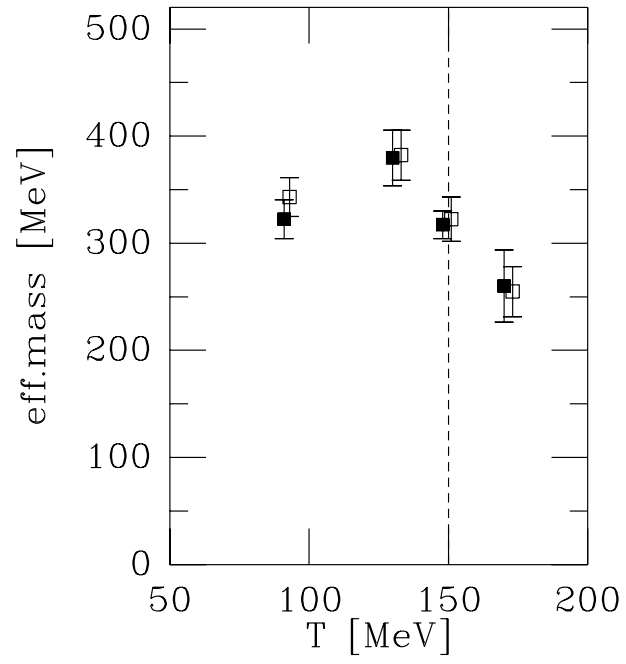


FIG. 5.

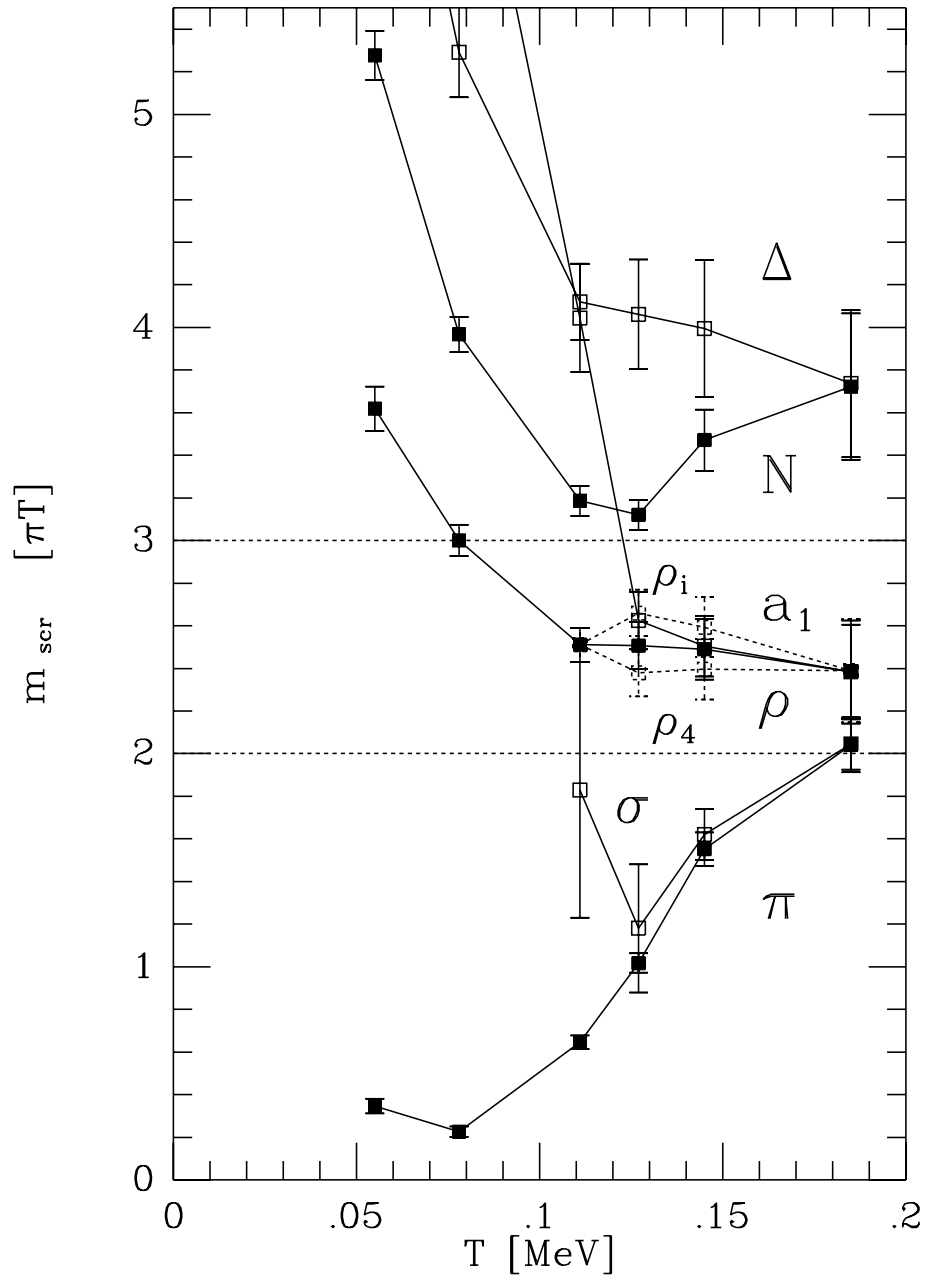


FIG. 6.

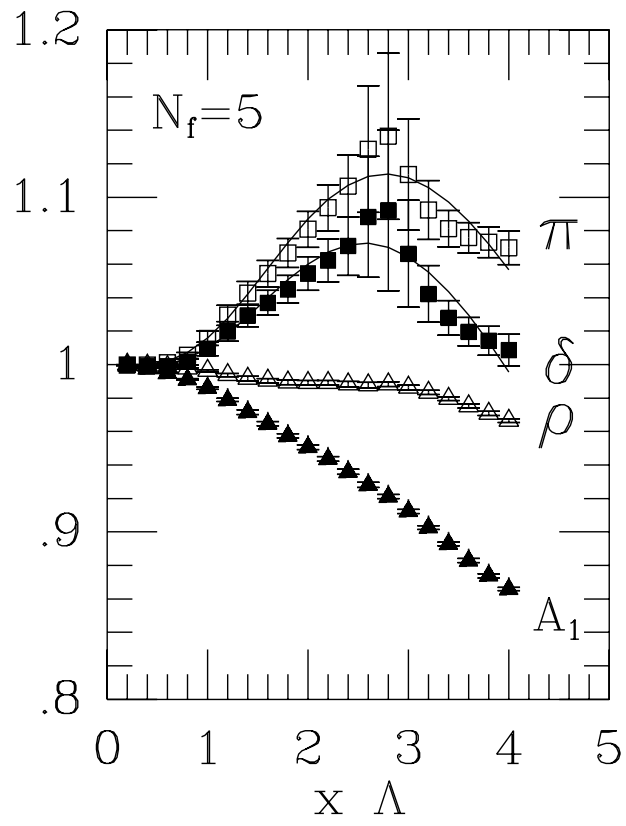


FIG. 7.